Potentiation of amyloid-β peptide neurotoxicity in human dental-pulp neuron-like cells by the membrane lipid peroxidation product 4-hydroxynonenal.

Highlights

- HNE causes overexpression of CD36 and β1-integrin receptors on neuronal cells.
- Increased expression of these receptors enhanced intracellular accumulation of Aβ.
- Blocking these receptors prevented neuronal necrotic cell death by HNE plus Aβ.

Potentiation of amyloid-β peptide neurotoxicity in human dental pulp neuron-like cells by the membrane lipid peroxidation product 4-hydroxynonenal

Gabriella Testa[a], Paola Gamba[a], Federica Di Scipio, Andrea Elio Sprio, Paolina Salamone, Simona Gargiulo, Barbara Sottero, Fiorella Biasi, Giovanni Nicolao Berta, Giuseppe Poli*, Gabriella Leonarduzzi

Department of Clinical and Biological Sciences, University of Turin, Orbassano (Turin), Italy.

*Correspondence to: G. Poli, Department of Clinical and Biological Sciences, Faculty of Medicine San Luigi Gonzaga, University of Turin, Regione Gonzole 10, 10043, Orbassano (Turin), Italy. Tel. +39 011 6705422; Fax: +39 011 6705424; *E-mail address*: giuseppe.poli@unito.it (G. Poli).

[a] These authors contributed equally to this work

ABSTRACT

Lipid peroxidation is generally considered as primarily implicated in the pathogenesis of Alzheimer's disease (AD); one of its more reactive end-products, 4-hydroxynonenal (HNE), has been shown to cause neuron dysfunction and degeneration. HNE production in the brain is stimulated by the amyloid-β peptide (Aβ), whose excessive accumulation in specific brain areas is a hallmark of AD. Conversely, Aβ production is up-regulated by this multifunctional aldehyde. Findings reported here point to the ability of HNE and Aβ to interact, with consequent potentiation of Aβ's cytotoxicity as determined *in vitro* using neuron-like cells derived from human dental-pulp progenitor cells. Preincubation of cells with the aldehyde markedly up-regulated Aβ uptake and intracellular accumulation, by overexpressing two of the three components of the plasma membrane multireceptor complex CD36/CD47/β1-integrin: experimental and clinical data indicate that intraneuronal accumulation of Aβ is an early event possibly playing a primary role in AD pathogenesis. That HNE-mediated over-expression of CD36 and β1-integrin, which plays a key role in HNE's potentiating Aβ neurotoxicity, in terms of necrosis, was confirmed when this effect was prevented by specific antibodies against the two receptors.

Keywords:
amyloid β, CD36 scavenger receptor, cell death, 4-hydroxynonenal

Introduction

Alzheimer's disease (AD), the most prevalent form of mental decline in developed countries, is characterized, from the neuropathological standpoint, by two hallmarks: intracellular neurofibrillary tangles made of hyperphosphorylated tau and extracellular deposits of amyloid β (Aβ) forming senile plaques. Moreover, the loss of neurons and synapses in the neocortex, hippocampus and other subcortical regions of the brain is a constant feature of this disease process [1,2].

With the exclusion of early-onset AD, which accounts for no more than 5-10% of total cases, the disease is the result of a complex interaction among a variety of acquired factors, acting on individuals with genetic predisposition (late-onset disease; 90-95% of total cases) [3-5]. Of these factors, lipid peroxidation, i.e. the oxidative breakdown of membrane polyunsaturated fatty acids (PUFA), is for a number of reasons generally considered as primarily implicated in both the initiation and the progression of AD. Firstly, the brain has a very high PUFA content and relatively low levels of naturally-occurring antioxidants, such as α-tocopherol, making it particularly sensitive to an increased steady-state of reactive oxygen species (ROS), a biochemical condition known as oxidative stress [6-10]. Further, various risk factors of late-onset AD, such as hypertension, smoking, diabetes mellitus, and inflammation, induce oxidative stress with peroxidation of cell-membrane lipids; through a positive feedback mechanism their pathological action is then amplified and sustained by oxidative stress [10,11].

Whether oxidative stress and lipid peroxidation products are the cause or the consequence of AD-associated neuropathology has long been the subject of debate [12-15]. Oxidative stress may promote Aβ production [16] and contribute to the formation of amyloid plaques [17,18] and, conversely, Aβ can stimulate the production of ROS [19,20].

Oxidative breakdown of membrane lipids or circulating lipoproteins generates highly-reactive aldehydes, of which the most relevant to brain pathophysiology appears to be 4-hydroxynonenal (HNE). HNE's involvement in AD pathogenesis has been hypothesized, as it causes neuron dysfunction and degeneration [21,22]. Because elevated levels of HNE have been found in the brain of AD patients, in both neurofibrillary tangles and senile plaques, as well as in the cerebrospinal fluid, it has been proposed as a candidate biomarker of this neurodegenerative disease [23,24]. The involvement of HNE in AD pathogenesis is also supported by important *in vitro* findings, including Aβ's ability to trigger HNE production by neurons [25] and, conversely, HNE-dependent enhancement of Aβ production in neurons, through the up-regulation of both β- and γ-secretase expression and activity, enzymes involved in the amyloidogenic pathway [26,27].

We are of the opinion that, since AD is a multistep and multifactorial disease process that develops chronically, it would be reductive to consider the expression of this disease as a linear series of distinct events, without any interaction or feedback. Instead of attempting to determine which comes first in the

neuropathology of AD, between HNE and Aβ, we thus focused on possible interactions between the two compounds in inducing neurotoxic effects.

Very recently, another lipid oxidation product of interest in brain pathophysiology, namely 24-hydroxycholesterol (24-OH), was found to strongly potentiate the necrogenic effect of the $A\beta_{1-42}$ peptide in two different human neuronal cell lines. This potentiation was due to the oxysterol's ability to stimulate the binding of Aβ to neuronal cells, by up-regulating a cluster of membrane receptors, comprising β1-integrin, CD36 and CD47 [28].

It is noteworthy that HNE up-regulates CD36 in murine macrophages [29], and that this scavenger receptor favors the binding of Aβ peptides to cell plasma membranes [30-32]. We thus deemed it important to investigate whether HNE was able to: i) up-regulate CD36 in human neuronal cells; ii) enhance Aβ binding to those cells and its subsequent uptake; iii) potentiate Aβ-mediated neurotoxicity.
To date, *in vitro* studies on nervous system diseases, including AD, have lacked an adequate human-cell model, most of them using human adult neurons or tumor cell lines; the former are difficult to cultivate and standardize, while many of the latter are without proper neuronal morphology and expression of neuron-specific markers [33,34]. The use of stem/precursor cells may thus represent an innovative approach. In this connection, dental-pulp stem and progenitor cells are particularly eligible because of their neural crest-linked ontogenesis [35,36], high plasticity, and ability to differentiate towards neural lineages [37,38].

We here applied a precursor cell-based approach, comprising primary cultures of human dental-pulp progenitor cells (DPPC), which spontaneously differentiate to dental pulp neuron-like cells (DPNLC) *in vitro*. HNE was found to cause over-expression not only of CD36 but also of another component of the multireceptor complex that binds the Aβ peptide, namely β1-integrin. The up-regulation of these components allowed the neurotoxic peptide to accumulate in greater amounts within DPNLC, and to induce much more extensive necrotic cell death than occurred in cells challenged with Aβ alone.

Materials and methods

Cell culture and differentiation

In line with stipulations of the Ethics Committee of Turin University, DPPC were isolated from the impacted third molar of a 25-year old woman; dental pulp was digested, size-sieved and isolated as described elsewhere [39]. Cells were cultured in RPMI-1640 supplemented with 10% fetal calf serum, 100 U/ml penicillin G, 40 μg/ml gentamicin sulfate and 2.5 μg/ml amphotericin B (Sigma-Aldrich, St Louis, MO, USA) at 37 °C in a humidified 5% CO_2 atmosphere. DPPC spontaneously differentiated into DPNLC after two months in culture (about 20 passages), without any addition of pro-differentiating agents.

Cytochemical analysis

Cells were observed in culture by phase-contrast microscopy (Leica DMIL, Leica Microsystems GmbH, Wetzlar, Germany). DPPC/DPNLC were cultured on poly-D-lysine-coated coverslips and stained for cytochemical or immunocytochemical analysis. Some DPPC were stained with toluidine blue dye to better morphological features. Specific markers were evaluated by immunocytochemical analysis, to characterize DPPC as progenitor cells and DPNLC as neuron-like cells. DPPC and DPNLC were incubated with specific primary antibodies overnight at 4 °C, and then with appropriate secondary antibodies for 1 h at room temperature. Assessed primary antibodies are specific for: proto-oncogene cKit (CD117 or stem-cell-factor receptor, SCF-R) (1:50); vascular endothelial growth factor receptor FLK1 (CD309) (1:50) (BD Pharmingen, Franklin Lakes, NJ, USA); stem-cell antigen 1 (SCA1) (1:50) (Cederlane, Ontario, Canada); multidrug resistance protein 1 (MDR1) (1:1000); polysialylated-neural-cell adhesion molecule (PSA-NCAM) (1:1000); neuronal nuclei antigen (NeuN) (1:1000) (Chemicon, Darmstadt, Germany); and glial fribrillar acid protein (GFAP) (1:70) (Dako, Milano, Italy); CD36 (1:500) (Clone FA6-152; HyCult Biotechnology b.v., Uden, The Netherlands); β1-integrin (1:500) and CD47 (1:1000) (Clone 4B7R; Santa Cruz, Biotechnology Inc., Santa Cruz, CA, USA); Nuclei were counterstained, where possible, with propidium iodide (1 µg/ml). Images were acquired with a LSM 510 confocal laser microscope (Carl Zeiss, Jena, Germany) equipped with an inverted microscope with Plan-NEOFLUAR lenses.

Cell treatments

Cells were treated with 0.5 µM 24-OH (Steraloids, Newport, RI, USA) or 1 µM HNE (Alexis, Vinci-Biochem, Vinci, Firenze, Italy). Some cells were then treated with $A\beta_{1-42}$ (200 nM) (AnaSpec, Fremont, CA, USA). In certain experiments, cells were pretreated with anti-CD36 antibody (4 µg/ml) (Clone FA6-152; HyCult Biotechnology b.v.) or with anti-β1-integrin antibody (4 µg/ml) (Clone 4B7R; Santa Cruz, Biotechnology Inc.). Incubation times for all experiments are reported in the Result section and in the figure legends.

RNA extraction and cDNA synthesis

DPNLC total RNA was extracted using TRIzol Reagent (Applied Biosystems, Monza, Italy) following the manufacturer's instructions. RNA was dissolved in RNase-free water fortified with RNase inhibitors (RNase SUPERase-In; Ambion, Austin, TX, USA) and purified through a Deoxyribonuclease I kit (Fermentas International Inc., Burlington, Canada). The amount and purity (A260/A280 ratio) of the extracted RNA were assessed spectrophotometrically.

cDNA was synthesized by reverse transcription from 2 µg RNA with a commercial kit and random primers (High-Capacity cDNA Reverse Transcription Kit; Applied Biosystems) following the manufacturer's instructions.

mRNA expression by qualitative RT-PCR

Qualitative reverse transcriptase-polymerase chain reaction (RT-PCR) was carried out using 0.1 µg cDNA, 2.5 µl 10X PCR Buffer II (Roche Applied Science, Indianapolis, USA), 1.5 µl 25 mM $MgCl_2$, 0.5 µl 10 mM dNTP, 0.05 U/µl Taq DNA Polymerase (Fermentas) and 0.75 µl of each specific 10 µM primer (Sigma-Aldrich) to a final volume of 25 µl.

Specific primer sequences were: β3-tubulin (TUBB3) fwd 5'-GGATCAGCGTCTACTACAACGAG-3'; TUBB3 rev 5'-CTGAAGAGATGTCCAAAGGCCC-3'; nestin fwd 5'-GTCCATCCTCAGTGGGTCAGA-3'; nestin rev 5'-CCGATTGAGCTCCCACATCT-3'; neuronal nuclei (NeuN) fwd 5'-CCGAGTGATGACCAACAAGAAGAC-3'; NeuN rev 5'-CGTAGCCTCCATAAATCTCAGCAC-3'; neuron-specific enolase (NSE) fwd 5'-CGTTACTTAGGCAAAGGTGTCCTG-3'; NSE rev 5'-TTCTCAGTCCCATCCAACTCCA-3'. As positive control, cDNA extracted from a human glioma sample was employed.

mRNA expression by real-time RT–PCR

Singleplex real-time RT–PCR was performed on 30 ng of cDNA using TaqMan Gene Expression Assay kits prepared for human CD36, β1-integrin, CD47, and β2-microglobulin, TaqMan Fast Universal PCR Master Mix, and 7500 Fast Real-Time PCR System (Applied Biosystems). Negative controls did not include cDNA. The oligonucleotide sequences are not revealed by the manufacturer because of proprietary interests. The cycling parameters were as follows: 20 s at 95°C for AmpErase UNG activation, 3 s at 95°C for AmpliTaq Gold DNA polymerase activation, 40 cycles of 3 s at 95°C (melting), and 30 s at 60°C (annealing ⁄ extension). The fractional cycle number (Ct) at which fluorescence passes the threshold, in the amplification plot of fluorescence signal vs. cycle number, was determined for each gene considered. The results were then normalized to the expression of β2-microglobulin, as housekeeping gene. Relative quantification of target gene expression was achieved with a mathematical method proposed by Livak & Schmittgen (2001) [40].

Congo red staining

DPNLC were grown on glass slides and, after treatment, specimens were fixed in 4% formalin for 15 min at room temperature. Cells were washed with 0.01 M PBS and then stained with a fresh solution of 0.5% filtered Congo red (Sigma-Aldrich) at room temperature for 3 min. After several washes with

deionized water, slides were mounted in glycerol/distilled water (1:1) plus 0.1% sodium azide (Sigma-Aldrich) and then observed through a LSM 510 confocal laser microscopy system (Carl Zeiss).

Evaluation of $A\beta_{1-42}$ cellular accumulation by ELISA

After cell treatment with HNE or 24-OH, followed by $A\beta_{1-42}$ addition, whole-cell extracts were prepared in ice-cold lysing buffer (1 ml of PBS was added with 10 µl Triton X-100, 10 µl SDS 10%, 5 µl DTT 1 M, 6 µl PMSF 0.1%, 10 µl aprotinin) for 30 min and sonicated for 1 min. The lysates were then cleared by centrifugation at 17,860 g for 15 min. The protein concentration was measured following Bradford's method [41].

$A\beta_{1-42}$ levels were quantified using the Human/Rat βAmyloid (42) ELISA Kit (Wako Chemicals GmbH, Neuss, Germany) following the manufacturer's instructions.

Measurement of necrotic and apoptotic cell death

Cell viability was measured in terms of the release of the enzyme lactate dehydrogenase (LDH). LDH activity was measured using a photometrical assay based on the conversion of pyruvic acid to lactic acid by this enzyme, in the presence of reduced NADH in culture medium. Control and treated-cells values are expressed as percentages of total LDH released by untreated cells (100%), which were lysed with PBS plus 5% Triton X-100.

The rate of apoptosis was evaluated through 4,6-diamidino-2-phenylindole (DAPI) staining. To identify apoptotic nuclei, cells grown on glass coverslips were fixed and permeabilized with 95% cold ethanol for 5 min at room temperature, and then washed twice with 0.1 M PBS. Slides were then incubated for 30 min at room temperature in DAPI solution. After rinsing in PBS, cells were observed and photographed under a Zeiss Axiovert 200 M fluorescence microscope.

Statistical analysis

Data were analyzed statistically using one-way ANOVA with Bonferroni's post-test for multiple comparisons. Differences at $P < 0.05$ were considered statistically significant. Calculations were performed with GRAPHPAD INSTAT3 software (GraphPad Software Inc., San Diego, CA, USA).

Results

Morphological features and protein expression of dental-pulp progenitor cells (DPPC)

Under light microscopy, DPPC showed flat, spindle-shaped fibroblastoid morphology (Fig. 1A), with central round nuclei characterized by two or more nucleoli (Fig. 1B). Immunocytochemical analysis highlighted the presence of stem-cell antigens cKit (Fig. 1C), FLK1 (Fig. 1D), and SCA1 (Fig. 1F), as well as that of P-glycoprotein (MDR1) (Fig. 1E). This expression profile confirms the progenitor status of these cells.

Spontaneous neuronal commitment of DPPC

After DPPC spontaneous differentiation, they consistently showed a neuron-like shape (Fig. 2A). Qualitative RT-PCR analyses demonstrated that DPNLC express genes related to neuronal differentiated status, namely those coding for cytoskeleton components TUBB3 and nestin, NeuN, a neuron-specific nuclear protein, and NSE, a neuronal glycolytic isoenzyme (Fig. 2B). Moreover, DPNLC expressed neural antigens, namely PSA-NCAM (Fig. 2C) and GFAP (Fig. 2D), besides the "neuronal nuclei" antigen NeuN (Fig. 2E). Constitutive expression of the multireceptor complex components, comprising β1-integrin (Fig. 2F), CD36 (Fig. 2G) and CD47 (Fig. 2H), has been shown.

HNE up-regulates the expression of genes coding for CD36 and β1-integrin in human dental pulp-derived cells showing a neuron-like phenotype (DPNLC)

After 4 h incubation, a single addition of the lipid peroxidation product HNE (final concentration 1 μM) to DPNLC induced a net increase in cell expression of the scavenger receptor CD36. At the same concentration, the aldehyde consistently and significantly also doubled the expression of β1-integrin, without exerting any effect on CD47 receptor (Fig. 3A). As a positive control, other DPNLC were challenged with 24-OH, i.e the oxysterol previously shown to up-regulate the same two plasma membrane proteins in human neuronal cell lines [28]. 24-OH (final concentration 0.5 μM) efficiently induced CD36 and β1-integrin also in human DPNLC, again without any effect on CD47 (Fig. 3B).

HNE enhances the internalization of $A\beta_{1-42}$ in DPNLC

The consequences of the increased expression of CD36 and β1-integrin, induced by HNE, were then investigated in DPNLC incubated for 48 h in the presence or otherwise of 1 μM HNE, and then challenged for 8 h with 200 nM $A\beta_{1-42}$. The same time scale applied in a previous study for 24-OH-modulated Aβ binding to neuronal cells [28] was employed here. As Fig. 4 shows, cell treatment with a single dose of HNE (1 μM) plus $A\beta_{1-42}$ led to much more marked internalization of the toxic peptide then occurred when cells were incubated with $A\beta_{1-42}$ alone, in the absence of HNE. Of note, cell treatment with 24-OH (0.5 μM) plus $A\beta_{1-42}$ also caused a pronounced intracellular accumulation of the

peptide. As reported in Table 1, $A\beta_{1-42}$ intracellular levels resulted to be about two-fold higher in both HNE or 24-OH treated cells versus untreated cells.

HNE potentiates $A\beta_{1-42}$-induced irreversible damage in DPNLC

With the aim of determining whether enhanced accumulation of toxic $A\beta_{1-42}$ in neuronal cells might potentiate the peptide's toxic effects, DPNLC were first incubated for 48 h with a single dose of 1 μM HNE, and then for a further 24 h with 200 nM $A\beta_{1-42}$ peptide. At the end of the experiment, necrotic cell death was evaluated, by measuring the extracellular percentage of LDH. As shown in Fig. 5A, in cells challenged with $A\beta_{1-42}$ for 24 h, LDH release increased about two-fold compared to untreated cells; cell treatment with HNE prior to $A\beta_{1-42}$ addition markedly potentiated the latter's neurotoxic effect.

Further, to evaluate the role of the HNE-induced up-regulation of membrane CD36 and β1-integrin in potentiating $A\beta_{1-42}$-induced cell necrosis, batches of HNE-treated cells were incubated for 1 h with either anti-CD36 or anti-β1-integrin specific antibodies, prior to the addiction of $A\beta_{1-42}$. Blocking these receptors not only prevented HNE-dependent enhancement of $A\beta_{1-42}$ neurotoxicity, but also blocked any increase of cell LDH leakage due to $A\beta_{1-42}$ treatment *per se* (Fig. 5A). In agreement with data previously obtained with neuronal cell lines [28], DPNLC treatment with 24-OH, used as positive control, gave the same results achieved with HNE (Fig. 5B).

A potential enhancement of Aβ's pro-apoptotic effect by the two compounds was also investigated: neither HNE nor 24-OH appeared to induce Aβ's apoptotic cell death as observed by DAPI staining (Fig. 6).

Discussion

Accumulation of Aβ peptides is thought to be an early and causative event in AD pathogenesis, and it increases markedly with disease progression [42]. Of the several intertwined causative factors that contribute to the development of AD, oxidative stress and the consequent pathological increase of membrane lipid peroxidation have been the subject of much consideration over recent years [1]. Thus, there is much focus on possible roles of lipid peroxidation-derived aldehydes in contributing to neuronal dysfunction in this neurodegenerative disease.

Among such aldehydes, HNE has become the most studied cytotoxic end product of lipid peroxidation and appears to be a main signaling molecule in the pathogenesis of AD. It has been demonstrated, indeed, to accumulate in relatively large amounts in brain cells, both with aging and with AD progression [22]. HNE has three functional groups that frequently act synergistically, and thus can undergo several reactions, especially with biomolecules containing amino and thiol groups. Quantitatively, proteins and peptides are the most important group of biomolecules targeted by HNE. It

has been estimated that 1-8% of HNE formed in cells has the ability to modify proteins [43]. In this connection, in autoptic samples from persons with mild cognitive impairment or early AD, liquid chromatography-mass spectrometry consistently detected 2-3 μmol HNE/g protein in the temporal cortex and hippocampus [24]; this post-mortem evidence of elevated levels of HNE-protein adducts in the hippocampus of such individuals has been confirmed in other studies [44]. Besides HNE, other aldehydes, such as trans-4-hydroxy-2-hexenal (HHE), 4-oxo-trans-2-nonenal (4-ONE), malondialdehyde (MDA) and acrolein, are well recognized neurotoxic agents [45,46]. HHE, like HNE, is an active biochemical mediator [47] and levels of HHE-protein adducts are increased in multiple brain regions in the progression of AD. Moreover, a time- and concentration-dependent decrease in survival was observed in primary cortical cultures treated with HHE [48]. Further, acrolein has been found to be elevated in hippocampus and temporal cortex where oxidative stress is high. It makes adducts with nucleophilic groups found on biomolecules and it causes cell death of hippocampal neurons [49,50].

Focusing on HNE, this aldehyde may be neurotoxic, acting through a variety of biochemical pathways, including the perturbation of cell signaling pathways [22,43,51,52]. In addition, HNE possesses a strong pro-inflammatory effect, operating, possibly among other mechanisms, by up-regulating the macrophagic expression and synthesis of cytokines, namely interleukin (IL)-1β and IL-8, tumor necrosis factor α (TNFα), transforming growth factor β1 (TGFβ1) and monocyte chemotactic protein-1 (MCP-1) [43, Poli et al., unpublished results]. HNE might also contribute to the inflammatory response of the AD brain, since this aldehyde has been identified as potential inducer of cyclooxygenase-2 [53]. Moreover, up-regulation of inflammatory molecules, including cyclooxygenase-2, has also been observed in the neuronal cell lines SK-N-BE and SH-SY-5Y (Poli et al., unpublished results). As already mentioned in the introduction, Aβ has been demonstrated to markedly up-regulate HNE steady-state levels in the brain [54,55]. Conversely, this hydroxyalkenal appears to stimulate the synthesis of toxic Aβ peptides, essentially $A\beta_{1-42}$, by promoting various steps of the synthesis process in neuronal cells [26,27]. Thus, a loop exists between HNE and Aβ as regards formation of the two compounds, but no evidence had thus far been reported about the pathological consequence of an interaction between them.

The neurotoxic interaction between HNE and $A\beta_{1-42}$ reported here is clearly based on the expression of CD36, a class B scavenger receptor, on the surface of neuronal cells. This plasma-membrane receptor has been confirmed as the key player molecule in the binding and internalization of Aβ by neuronal cells [32]. In microglial cells, the CD36 receptor is reported to form a multicomplex receptor with CD47 and β1-integrin, able to bind monomers and amyloid fibrils [56], and this receptor complex was recently also reported to be involved in 24-OH-induced $A\beta_{1-42}$ binding by human neuronal cell lines, namely differentiated SK-N-BE and NT-2 cells [28].

The present findings suggest that, in progenitor cells obtained from human dental pulp differentiated towards the neuronal phenotype (Fig. 2), HNE, like 24-OH, may stimulate expression of the same

multicomplex receptor (CD36/CD47/β1-integrin) (Fig. 3). While over-expression of CD36 by HNE has already been reported, but in macrophage cells [29], up-regulation of β1-integrin by this aldehyde appears to be a new finding.

Of note, CD36-depending signaling has also been implicated in the pro-inflammatory effects of endogenous ligands, such as oxidized low density lipoprotein (oxLDL), oxidized lipids and Aβ. Signals from the scavenger receptor CD36 might, indeed, regulate assembly and activation of Toll-like receptor (TLR) 4 and 6 heterodimers, leading to sterile inflammation [57]. TLR4 expression has been demonstrated to increase in neurons when exposed to HNE or Aβ and to contribute to the neuronal degeneration in AD [58]. We could, thus, hypothesize that activation of CD36/TLR4/TLR6 might be a pro-inflammatory trigger common to oxLDL, Aβ, and HNE.

Importantly, a growing body of evidence from different transgenic models, *in vitro* as well as clinical studies, strongly suggests that intraneuronal accumulation of Aβ is an early event, and might play a primary role in the pathogenesis of AD [59,60]. Oxidative stress has been found to induce the uptake of Aβ, administered extracellularly to neuronal cells, and its localization to the nucleus [61-64]. Here we provide clear evidence that a single physiopathologically-compatible dose of HNE markedly enhances intraneuronal, followed by intranuclear, accumulation of Aβ.

Instead of using immortalized neuronal cell lines, which often lack adequate neuronal morphology and expression of neuron-specific markers, and that often consist of non-uniform cells, we preferred here to employ a much more uniform population of neuron-like cells, i.e. those obtainable from the differentiation of stem cells. In this connection, dental-pulp mesenchymal stem cells appeared to be the best choice. Besides being readily accessible, these cells originate from the cranial neural crest [35,36], they possess great plasticity, express some neural markers, are capable of forming neurospheres, and, in particular, they can spontaneously differentiate along the neural lineage *in vitro* [37,38].

As reported in Fig. 5, addition of a standard amount of the peptide $A\beta_{1-42}$ *per se* induced some degree of necrotic death, measured in terms of LDH release. Cell dosing with HNE also determined a moderate increase of LDH in the cell suspension medium. However, when the two treatments were combined, the neurotoxicity index reached values above the sum of the two separate necrogenic effects. Notably, cell treatment with antibodies against either CD36 or β1-integrin restored LDH release to values measured in neuronal cells incubated throughout the experimental time in the absence of HNE and Aβ. The latter finding would suggest that the rate of cell death occurring in the presence of $A\beta_{1-42}$ alone may also be dependent on the constitutive expression of some amount of the multicomplex receptor that includes CD36 and β1-integrin. The moderate but positive Congo red staining, shown by DPNLC challenged with $A\beta_{1-42}$ alone, indirectly confirms this hypothesis (Fig. 4), as well as the quantification of $A\beta_{1-42}$ intracellular levels by ELISA (Table 1). In contrast, the different compounds did not show any apoptotic effect on treated cells (Fig. 6).

Figure 7 summarizes: i) the sequence of events underlying the observed neurotoxic interaction of HNE and Aβ peptide, and ii) the complete prevention of necrotic cell death by the specific receptor

blockade. As regards the mechanisms whereby HNE might potentiate $A\beta_{1-42}$ toxicity against neuronal cells, its binding to the amyloid peptides appears primary and essential. Although HNE is known to form adducts with three different side chains in proteins and peptides, including Aβ, namely Cys, His, and Lys [43], characterization of HNE-Aβ adducts by liquid chromatography/mass spectrometry suggests the localization of one or more moieties of the aldehyde in the region 6-16 of these adducts, a region comprising all three His residues of the Aβ peptide [65]. The reaction and interaction between HNE and Aβ occur mainly within the neuronal cells, since Aβ intracellular accumulation is prevented by blocking the multicomplex receptor located on the plasma membrane; moreover, HNE has been shown to reach different cytosolic compartments, including the nucleus, in many cell types [43]. However, the manner in which HNE-Aβ adducts, rather than either of the two molecules separately, modulate cell function and fate, in terms of signal transduction and gene transcription, is not yet entirely clear, and would thus deserve in-depth investigation in the future. Again in connection with the potentiation of Aβ's neurotoxicity by HNE, it may be considered that the addition reaction induced by this aldehyde most likely favors the formation of Aβ oligomers, thought to be the most toxic form of Aβ.

Abbreviations

(Aβ)	amyloid β
(AD)	Alzheimer's disease
(DAPI)	4,6-diamidino-2-phenylindole
(DPNLC)	dental-pulp neuron-like cells
(DPPC)	dental-pulp progenitor cells
(GFAP)	glial fibrillary acidic protein
(HHE)	trans-4-hydroxy-2-hexenal
(HNE)	4-hydroxynonenal
(IL)	interleukin
(LDH)	lactate dehydrogenase
(MCP-1)	monocyte chemotactic protein-1
(MDA)	malondialdehyde
(MDR1)	multidrug resistance protein 1
(N-CAM)	neural cell adhesion molecule
(NeuN)	neuronal nuclei
(NSE)	neuron-specific enolase
(24-OH)	24-hydroxycholesterol
(4-ONE)	4-oxo-trans-2-nonenal
(PSA-NCAM)	polysialylated-neural cell adhesion molecule
(PUFA)	polyunsaturated fatty acids

(ROS)	reactive oxygen species
(RT-PCR)	reverse transcriptase-polymerase chain reaction
(SCA1)	stem cell antigen 1
(TGFβ1)	transforming growth factor β1
(TNFα)	tumor necrosis factor α
(TUBB3)	β3-tubulin

Acknowledgments

The authors thank the Italian Ministry of University (Prin 2008 and 2009), the Piedmontese Regional Government (Ricerca Sanitaria Finalizzata 2009), the CRT Foundation, Turin, and the University of Turin, Italy, for supporting this work.

References

[1] Querfurth, H. W.; LaFerla, F. M. Alzheimer's disease. N. Engl. J. Med. 362:329-344; 2010.
[2] Chopra, K.; Misra, S.; Kuhad, A. Neurobiological aspects of Alzheimer's disease. Expert. Opin. Ther. Targets 15:535-555; 2011.
[3] Rossor, M. N.; Fox, N. C.; Freeborough, P. A.; Harvey, R. J. Clinical features of sporadic and familial Alzheimer's disease. Neurodegeneration 5:393-397; 1996.
[4] Tanzi, R. E.; Bertram, L. New frontiers in Alzheimer's disease genetics. Neuron 32:181-184; 2001.
[5] Querfurth, H. W.; LaFerla, F. M. Alzheimer's disease. N. Engl. J. Med. 362:329-344; 2010.
[6] Jeandel, C.; Nicolas, M. B.; Dubois, F.; Nabet-Belleville, F.; Penin, F.; Cuny, G. Lipid peroxidation and free radical scavengers in Alzheimer’s disease. Gerontology 35:275-282; 1989.
[7] Zaman, Z.; Roche, S.; Fielden, P.; Frost, P. G.; Niriella, D. C.; Cayley, A. C. Plasma concentrations of vitamins A and E and carotenoids in Alzheimer’s disease. Age Ageing 21:91-94; 1992.
[8] Arca, M.; Natoli, S.; Micheletta, F.; Riggi, S.; Di Angelantonio, E.; Montali, A.; Antonini, T. M.; Antonini, R.; Diczfalusy, U.; Iuliano, L. Increased plasma levels of oxysterols, in vivo markers of oxidative stress, in patients with familial combined hyperlipidemia: reduction during atorvastatin and fenofibrate therapy. Free Radic. Biol. Med. 42:698-705; 2007.
[9] Long, E. K.; Picklo, M. J. Sr. Trans-4-hydroxy-2-hexenal, a product of n-3 fatty acid peroxidation: make some room HNE... Free Radic. Biol. Med. 49:1-8; 2010.
[10] Axelsen, P. H.; Komatsu, H.; Murray, I. V. Oxidative stress and cell membranes in the pathogenesis of Alzheimer's disease. Physiology (Bethesda) 26:54-69; 2011.

[11] Murray, I. V.; Proza, J. F.; Sohrabji, F.; Lawler, J. M. Vascular and metabolic dysfunction in Alzheimer's disease: a review. Exp. Biol. Med. (Maywood) 236:772-782; 2011.

[12] Nunomura, A.; Perry, G.; Aliev, G.; Hirai, K.; Takeda, A.; Balraj, E. K.; Jones, P. K.; Ghanbari, H.; Wataya, T.; Shimohama, S.; Chiba, S.; Atwood, C. S.; Petersen, R. B.; Smith, M. A. Oxidative damage is the earliest event in Alzheimer disease. J. Neuropathol. Exp. Neurol. 60:759-767; 2001.

[13] Zhu, X.; Su, B.; Wang, X.; Smith, M. A.; Perry, G. Causes of oxidative stress in Alzheimer disease. Cell. Mol. Life Sci. 64:2202-2210; 2007.

[14] Smith, M. A.; Zhu, X.; Tabaton, M.; Liu, G.; McKeel, D. W. Jr.; Cohen, M. L.; Wang, X., Siedlak, S. L.; Dwyer, B. E.; Hayashi, T.; Nakamura, M.; Nunomura, A.; Perry, G. Increased iron and free radical generation in preclinical Alzheimer disease and mild cognitive impairment. J. Alzheimers Dis. 19:363-372; 2010.

[15] Bonda, D. J.; Wang, X.; Perry, G.; Nunomura, A.; Tabaton, M.; Zhu, X.; Smith, M. A. Oxidative stress in Alzheimer disease: a possibility for prevention. Neuropharmacology 59:290-294; 2010.

[16] Naylor, R.; Hill, A. F.; Barnham, K. J. Neurotoxicity in Alzheimer's disease: is covalently crosslinked A beta responsible? Eur. Biophys. J. 37:265-268; 2008.

[17] Paola, D.; Domenicotti, C.; Nitti, M.; Vitali, A.; Borghi, R.; Cottalasso, D.; Zaccheo, D.; Odetti, P.; Strocchi, P.; Marinari, U. M.; Tabaton, M.; Pronzato, M. A. Oxidative stress induces increase in intracellular amyloid beta-protein production and selective activation of betaI and betaII PKCs in NT2 cells. Biochem. Biophys. Res. Commun. 268:642-246; 2000.

[18] Praticò, D.; Uryu, K.; Leight, S.; Trojanoswki, J. Q.; Lee, V. M. Increased lipid peroxidation precedes amyloid plaque formation in an animal model of Alzheimer amyloidosis. J. Neurosci. 21:4183-4187; 2001.

[19] Harkany, T.; Abrahám, I.; Kónya, C.; Nyakas, C.; Zarándi, M.; Penke, B.; Luiten, P. G. Mechanisms of beta-amyloid neurotoxicity: perspectives of pharmacotherapy. Rev. Neurosci. 11:329-382; 2000.

[20] Ding, Q.; Dimayuga, E.; Keller, J. N. Oxidative damage, protein synthesis, and protein degradation in Alzheimer's disease. Curr. Alzheimer Res. 4:73-79; 2007.

[21] Mattson, M. P. Pathways towards and away from Alzheimer's disease. Nature 430:631-639; 2004.

[22] Mattson, M. P. Roles of the lipid peroxidation product 4-hydroxynonenal in obesity, the metabolic syndrome, and associated vascular and neurodegenerative disorders. Exp. Gerontol. 44:625-633; 2009.

[23] Wang, D. S.; Iwata, N.; Hama, E.; Saido, T. C.; Dickson, D. W. Oxidized neprilysin in aging and Alzheimer's disease brains. Biochem. Biophys. Res. Commun. 310:236-241; 2003.

[24] Williams, T. I.; Lynn, B. C.; Markesbery, W. R.; Lovell, M. A. Increased levels of 4-hydroxynonenal and acrolein, neurotoxic markers of lipid peroxidation, in the brain in Mild Cognitive Impairment and early Alzheimer's disease. Neurobiol. Aging 27:1094-1099; 2006.

[25] Butterfield, D. A.; Galvan, V.; Lange, M. B.; Tang, H.; Sowell, R. A.; Spilman, P.; Fombonne, J.; Gorostiza, O.; Zhang, J.; Sultana, R.; Bredesen, D. E. In vivo oxidative stress in brain of Alzheimer

disease transgenic mice: Requirement for methionine 35 in amyloid beta-peptide of APP. Free Radic. Biol. Med. 48:136-144; 2010.

[26] Tamagno, E.; Parola, M.; Bardini, P.; Piccini, A.; Borghi, R.; Guglielmotto, M.; Santoro, G.; Davit, A.; Danni, O.; Smith, M. A.; Perry, G.; Tabaton, M. Beta-site APP cleaving enzyme up-regulation induced by 4-hydroxynonenal is mediated by stress-activated protein kinases pathways. J. Neurochem. 92:628-936; 2005.

[27] Jo, D. G.; Arumugam, T. V.; Woo, H. N.; Park, J. S.; Tang, S. C.; Mughal, M.; Hyun, D. H.; Park, J. H.; Choi, Y. H.; Gwon, A. R.; Camandola, S.; Cheng, A.; Cai, H.; Song, W.; Markesbery, W. R.; Mattson, M. P. Evidence that gamma-secretase mediates oxidative stress-induced beta-secretase expression in Alzheimer's disease. Neurobiol. Aging 31:917-925; 2010.

[28] Gamba, P.; Leonarduzzi, G.; Tamagno, E.; Guglielmotto, M.; Testa, G.; Sottero, B.; Gargiulo, S.; Biasi, F.; Mauro, A.; Viña, J.; Poli, G. Interaction between 24-hydroxycholesterol, oxidative stress, and amyloid-β in amplifying neuronal damage in Alzheimer's disease: three partners in crime. Aging Cell 10:403-417; 2011.

[29] Yun, M. R.; Im, D. S.; Lee, S. J.; Park, H. M.; Bae, S. S.; Lee, W. S.; Kim, C. D. 4-Hydroxynonenal enhances CD36 expression on murine macrophages via p38 MAPK-mediated activation of 5-lipoxygenase. Free Radic. Biol. Med. 46:692-698; 2009.

[30] Bamberger, M. E.; Harris, M. E.; McDonald, D. R.; Husemann, J.; Landreth, G. E. A cell surface receptor complex for fibrillar beta-amyloid mediates microglial activation. J. Neurosci. 23:2665-2674; 2003.

[31] Stewart, C. R.; Stuart, L. M.; Wilkinson, K.; van Gils, J. M.; Deng, J.; Halle, A.; Rayner, K. J.; Boyer, L.; Zhong, R.; Frazier, W. A.; Lacy-Hulbert, A.; El Khoury, J.; Golenbock, D. T.; Moore, K. J. CD36 ligands promote sterile inflammation through assembly of a Toll-like receptor 4 and 6 heterodimer. Nat. Immunol. 11:155-161; 2010.

[32] Park, L.; Wang, G.; Zhou, P.; Zhou, J.; Pitstick, R.; Previti, M. L.; Younkin, L.; Younkin, S. G.; Van Nostrand, W. E.; Cho, S.; Anrather, J.; Carlson, G. A.; Iadecola, C. Scavenger receptor CD36 is essential for the cerebrovascular oxidative stress and neurovascular dysfunction induced by amyloid-beta. Proc. Natl. Acad. Sci. U S A 108:5063-5068; 2011.

[33] Aksenova, M. V.; Aksenov, M. Y.; Mactutus, C. F.; Booze, R. M. Cell culture models of oxidative stress and injury in the central nervous system. Curr. Neurovasc. Res. 2:73-89; 2005.

[34] Agholme, L.; Lindström, T.; Kågedal, K.; Marcusson, J.; Hallbeck, M. An in vitro model for neuroscience: differentiation of SH-SY5Y cells into cells with morphological and biochemical characteristics of mature neurons. J. Alzheimers Dis. 20:1069-1082; 2010.

[35] Chai, Y.; Jiang, X.; Ito, Y.; Bringas, P. Jr.; Han, J.; Rowitch, D. H.; Soriano, P.; McMahon, A. P.; Sucov, H. M. Fate of the mammalian cranial neural crest during tooth and mandibular morphogenesis. Development 127:1671-1679; 2000.

[36] Rothová, M.; Feng, J.; Sharpe, P. T.; Peterková, R.; Tucker, A. S. Contribution of mesoderm to the developing dental papilla. Int. J. Dev. Biol. 55:59-64; 2011.

[37] Huang, G. T.; Gronthos, S.; Shi, S. Mesenchymal stem cells derived from dental tissues vs. those from other sources: their biology and role in regenerative medicine. J. Dent. Res. 88:792-806; 2009.

[38] Sprio, A. E.; Di Scipio, F.; Raimondo, S.; Salamone, P.; Pagliari, F.; Pagliari, S., Folino, A.; Forte, G.; Geuna, S.; Di Nardo, P.; Berta, G. N. Self-Renewal and Multipotency Coexist in a Long-Term Cultured Adult Rat Dental Pulp Stem Cell Line: An Exception to the Rule? Stem Cells Dev. In press; 2012.

[39] Gronthos, S.; Mankani, M.; Brahim, J.; Robey, P. G.; Shi, S. Postnatal human dental pulp stem cells (DPSCs) in vitro and in vivo. Proc. Natl. Acad. Sci. U S A 97:13625-13630; 2000.

[40] Livak, K. J.; Schmittgen, T. D. Analysis of relative gene expression data using real-time quantitative PCR and the 2(-Delta Delta C(T)) Method. Methods 25:402-408; 2001.

[41] Bradford, M. M. A rapid and sensitive method for the quantitation of microgram quantities of protein utilizing the principle of protein-dye binding. Anal. Biochem. 72:248-254; 1976.

[42] Selkoe, D. J. Amyloid beta-protein precursor: new clues to the genesis of Alzheimer's disease. Curr. Opin. Neurobiol. 4:708-716; 1994.

[43] Poli, G.; Schaur, R. J.; Siems, W. G.; Leonarduzzi, G. 4-hydroxynonenal: a membrane lipid oxidation product of medicinal interest. Med. Res. Rev. 28:569-631; 2008.

[44] Butterfield, D. A.; Reed, T.; Perluigi, M.; De Marco, C.; Coccia, R.; Cini, C.; Sultana, R. Elevated protein-bound levels of the lipid peroxidation product, 4-hydroxy-2-nonenal, in brain from persons with mild cognitive impairment. Neurosci. Lett. 397:170-173; 2006.

[45] Jomova, K.; Vondrakova, D.; Lawson, M.; Valko, M. Metals, oxidative stress and neurodegenerative disorders. Mol. Cell. Biochem. 345:91-104; 2010.

[46] Butterfield, D. A.; Bader Lange, M. L.; Sultana, R. Involvements of the lipid peroxidation product, HNE, in the pathogenesis and progression of Alzheimer's disease Biochim. Biophys. Acta. 1801:924-929; 2010.

[47] Long, E. K.; Picklo, M. J. Sr. Trans-4-hydroxy-2-hexenal, a product of n-3 fatty acid peroxidation: make some room HNE... Free Radic. Biol. Med. 49:1-8; 2010.

[48] Bradley, M. A.; Xiong-Fister, S.; Markesbery, W. R.; Lovell, M. A. Elevated 4-hydroxyhexenal in Alzheimer's disease (AD) progression. Neurobiol. Aging 33:1034-1044; 2012.

[49] Dang, T. N.; Arseneault, M.; Murthy, V.; Ramassamy, C. Potential role of acrolein in neurodegeneration and in Alzheimer's disease. Curr. Mol. Pharmacol. 3:66-78; 2010.

[50] Singh, M.; Dang, T. N.; Arseneault, M.; Ramassamy, C. Role of by-products of lipid oxidation in Alzheimer's disease brain: a focus on acrolein. J. Alzheimers Dis. 21:741-756; 2010.

[51] Keller, J. N.; Mattson, M. P. Roles of lipid peroxidation in modulation of cellular signaling pathways, cell dysfunction, and death in the nervous system. Rev. Neurosci. 9:105-116; 1998.

[52] Perry, G.; Castellani, R. J.; Hirai, K.; Smith, M. A. Reactive Oxygen Species Mediate Cellular Damage in Alzheimer Disease. J. Alzheimers Dis. 1:45-55; 1998.

[53] Uchida, K. A lipid-derived endogenous inducer of COX-2: a bridge between inflammation and oxidative stress. Mol. Cells 25:347-351; 2008.

[54] Butterfield, D. A.; Lauderback, C. M. Lipid peroxidation and protein oxidation in Alzheimer's disease brain: potential causes and consequences involving amyloid beta-peptide-associated free radical oxidative stress. Free Radic. Biol. Med. 32:1050-1060; 2002.

[55] Abdul, H. M.; Sultana, R.; St Clair, D. K.; Markesbery, W. R.; Butterfield, D. A. Oxidative damage in brain from human mutant APP/PS-1 double knock-in mice as a function of age. Free Radic. Biol. Med. 45:1420-1425; 2008.

[56] Bamberger, M. E.; Harris, M. E.; McDonald, D. R.; Husemann, J.; Landreth, G. E. A cell surface receptor complex for fibrillar beta-amyloid mediates microglial activation. J. Neurosci. 23:2665-2674; 2003.

[57] Stewart, C. R.; Stuart, L. M.; Wilkinson, K.; van Gils, J. M.; Deng, J.; Halle, A.; Rayner, K. J.; Boyer, L.; Zhong, R.; Frazier, W. A.; Lacy-Hulbert, A.; El Khoury, J.; Golenbock, D. T.; Moore, K. J. CD36 ligands promote sterile inflammation through assembly of a Toll-like receptor 4 and 6 heterodimer. Nat. Immunol. 11:155-161; 2010.

[58] Tang, S. C.; Lathia, J. D.; Selvaraj, P. K.; Jo, D. G.; Mughal, M. R.; Cheng, A.; Siler, D. A.; Markesbery, W. R.; Arumugam, T. V.; Mattson, M. P. Toll-like receptor-4 mediates neuronal apoptosis induced by amyloid beta-peptide and the membrane lipid peroxidation product 4-hydroxynonenal. Exp. Neurol. 213:114-121; 2008.

[59] Mohamed, A.; Posse de Chaves, E. Aβ internalization by neurons and glia. Int. J. Alzheimers Dis. 2011:127984. 2011.

[60] Wirths, O.; Bayer, T. A. Intraneuronal Aβ accumulation and neurodegeneration: Lessons from transgenic models. Life Sci. In press; 2012.

[61] Ohyagi, Y.; Asahara, H.; Chui, D. H.; Tsuruta, Y.; Sakae, N.; Miyoshi, K.; Yamada, T.; Kikuchi, H.; Taniwaki, T.; Murai, H.; Ikezoe, K.; Furuya, H.; Kawarabayashi, T.; Shoji, M.; Checler, F.; Iwaki, T.; Makifuchi, T.; Takeda, K.; Kira, J.; Tabira, T. Intracellular Abeta42 activates p53 promoter: a pathway to neurodegeneration in Alzheimer's disease. FASEB J. 19:255-257; 2005.

[62] Ohyagi, Y.; Tabira, T. Intracellular amyloid beta-protein and its associated molecules in the pathogenesis of Alzheimer's disease. Mini Rev. Med. Chem. 6:1075-1080; 2006.

[63] Ohyagi, Y. Intracellular amyloid beta-protein as a therapeutic target for treating Alzheimer's disease. Curr. Alzheimer Res. 5:555-561; 2008.

[64] Bailey, J. A.; Maloney, B.; Ge, Y. W.; Lahiri, D. K. Functional activity of the novel Alzheimer's amyloid β-peptide interacting domain (AβID) in the APP and BACE1 promoter sequences and implications in activating apoptotic genes and in amyloidogenesis. Gene 488:13-22; 2011.

[65] Magni, F.; Galbusera, C.; Tremolada, L.; Ferrarese, C.; Kienle, M. G. Characterisation of adducts of the lipid peroxidation product 4-hydroxy-2-nonenal and amyloid beta-peptides by liquid chromatography/electrospray ionisation mass spectrometry. Rapid. Commun. Mass Spectrom. 16:1485-1493; 2002.

Figure legends

Fig. 1. DPPC characterization before neural differentiation. Panel A: DPPC display a fibroblastoid shape, observed by phase-contrast microscopy; panel B: cell shape was highlighted by toluidine blue staining; panels C,D,E,F: DPPC express typical precursor markers, such as the proto-oncogene cKit (C), the vascular endothelial growth factor receptor FLK1 (D), the multidrug resistance protein MDR1 (E) and the stem cell antigen SCA1 (F), all observed by laser confocal microscopy as described in the Materials and methods. Bar length: 20 μm.

Fig. 2. Characterization of human dental-pulp-derived neuron-like cells (DPNLC). Panel A: DPNLC morphological aspect; panel B: mRNA expression of neuronal genes coding for cytoskeleton components β3-tubulin (TUBB3), nestin, neuron-specific enolase (NSE) and neuronal nuclei (NeuN) (+: positive control); panels C, D, E: synthesis of neural markers, namely polysialylated-neural cell adhesion molecule PSA-NCAM (C), glial fibrillary acidic protein GFAP (D) and neuronal nuclei NeuN (E); panels F, G, H: constitutive expression of the multireceptor complex components β1-integrin (F), CD36 (G) and CD47 (H). Bar length: 20 μm.

Fig. 3. Effect of 4-hydroxynonenal (HNE) (A) and 24-hydroxycholesterol (24-OH) (B) on the expression of CD36, β1-integrin and CD47. Gene expression was quantified by real-time RT-PCR in DPNLC treated for 4 h with 1 μM HNE or 0.5 μM 24-OH. Untreated cells were used as controls. Data, normalized to β2-microglobulin, are expressed as mean values ± standard deviation of three different experiments. ***$P < 0.001$ vs. control group.

Fig. 4. Congo red staining of amyloid-β internalization in DPNLC cells. Cells were treated with HNE (1 μM) or 24-OH (0.5 μM) for 48 h and then with $A\beta_{1\text{-}42}$ (200 nM) for 8 h. Other batches of cells were treated with $A\beta_{1\text{–}42}$ alone for 8 h. Untreated cells were used as controls. $A\beta_{1\text{-}42}$ cell internalization was observed by confocal laser microscopy: excitation 488-543 nm and emission 560 nm; lens 20 x⁄0.5, 3 x. Images are from one representative experiment of two experiments performed.

Fig. 5. Effect of 4-hydroxynonenal (HNE) and 24-hydroxycholesterol (24-OH) on lactate dehydrogenase (LDH) release. DPNLC cells were incubated for 48 h after a single initial addition of 1 μM HNE or 0.5 μM 24-OH, then in the presence or otherwise of 200 nM $A\beta_{1\text{-}42}$ for 24 h. Some cell aliquots,

immediately after HNE or 24-OH challenge, were incubated for 1 h in the presence of anti-CD36 (4 µg/ml) or anti-β1-integrin (4 µg/ml) specific antibodies, immediately prior to the 24 h treatment with $A\beta_{1-42}$. Untreated cells were taken as controls. Histograms report mean values ± standard deviation of three experiments. ***P < 0.001 vs. control group; §§§P < 0.001 vs. $A\beta_{1-42}$; ###P < 0.001 vs. HNE or 24-OH; †††P < 0.001 vs. HNE+$A\beta_{1-42}$ or 24-OH+ $A\beta_{1-42}$; ††P < 0.01 vs. 24-OH+ $A\beta_{1-42}$.

Fig. 6. Nuclear morphology study by DAPI staining in DPNLC cells treated with 4-hydroxynonenal (HNE) or 24-hydroxycholesterol (24-OH) for 48 h and then for 24 h with $A\beta_{1-42}$ (200 nM). Cells were examined using a fluorescence microscope (Zeiss Axiovert 200 M) with an ultraviolet filter and a 20x/0.30 lens.

Fig. 7. Schematic representation of the events underlying HNE/24-OH-dependent potentiation of amyloid β ($A\beta_{1-42}$) toxicity against human DPNLC. Cell treatment with a single initial dose of HNE (1 µM) or 24-OH (0.5 µM) (A) up-regulates the receptor complex CD36/β1-integrin/CD47 levels on the neuronal surface (B). As a consequence, binding and intracellular uptake of the externally-added $A\beta_{1-42}$ are favored, and neuronal death occurs (C). Amplification of $A\beta_{1-42}$ neurotoxic effect by the two lipid peroxidation products is fully prevented by treating neuronal cells with anti-CD36 or anti-β1-integrin specific antibodies (D).

Fig.1

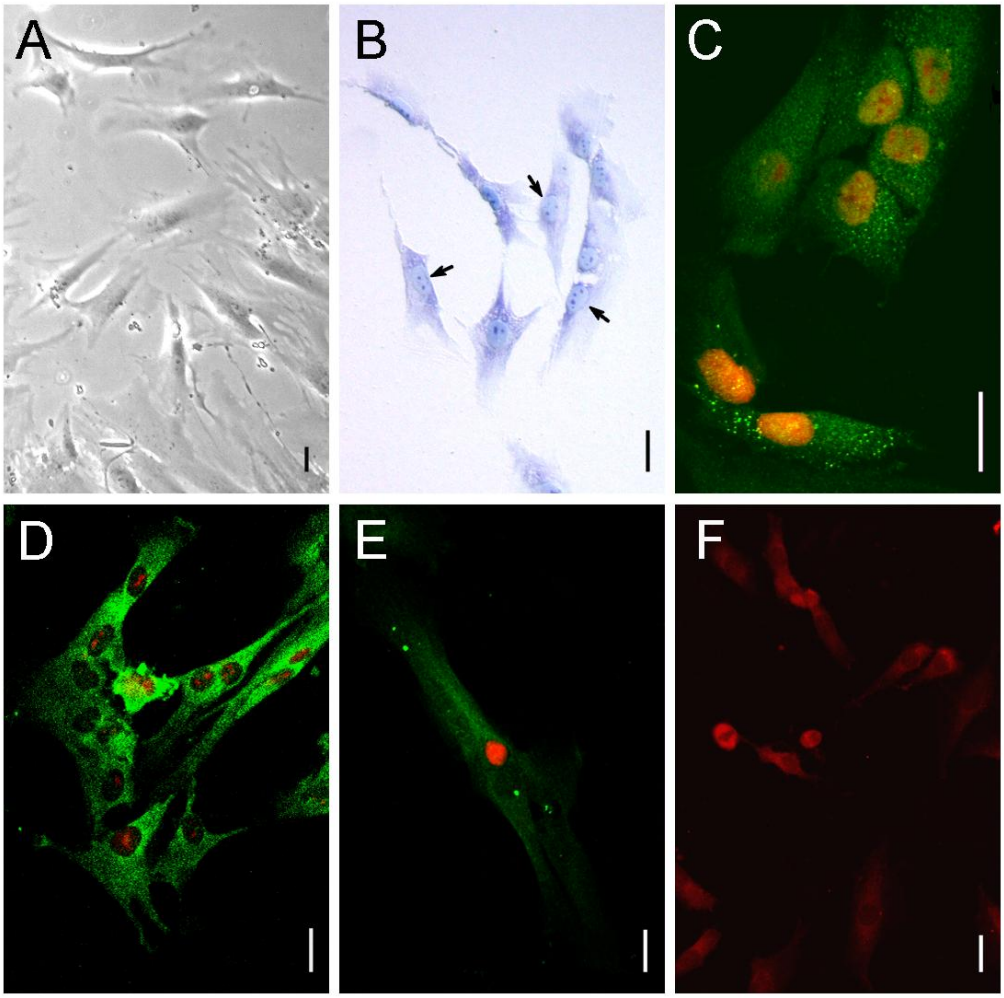

Fig.2

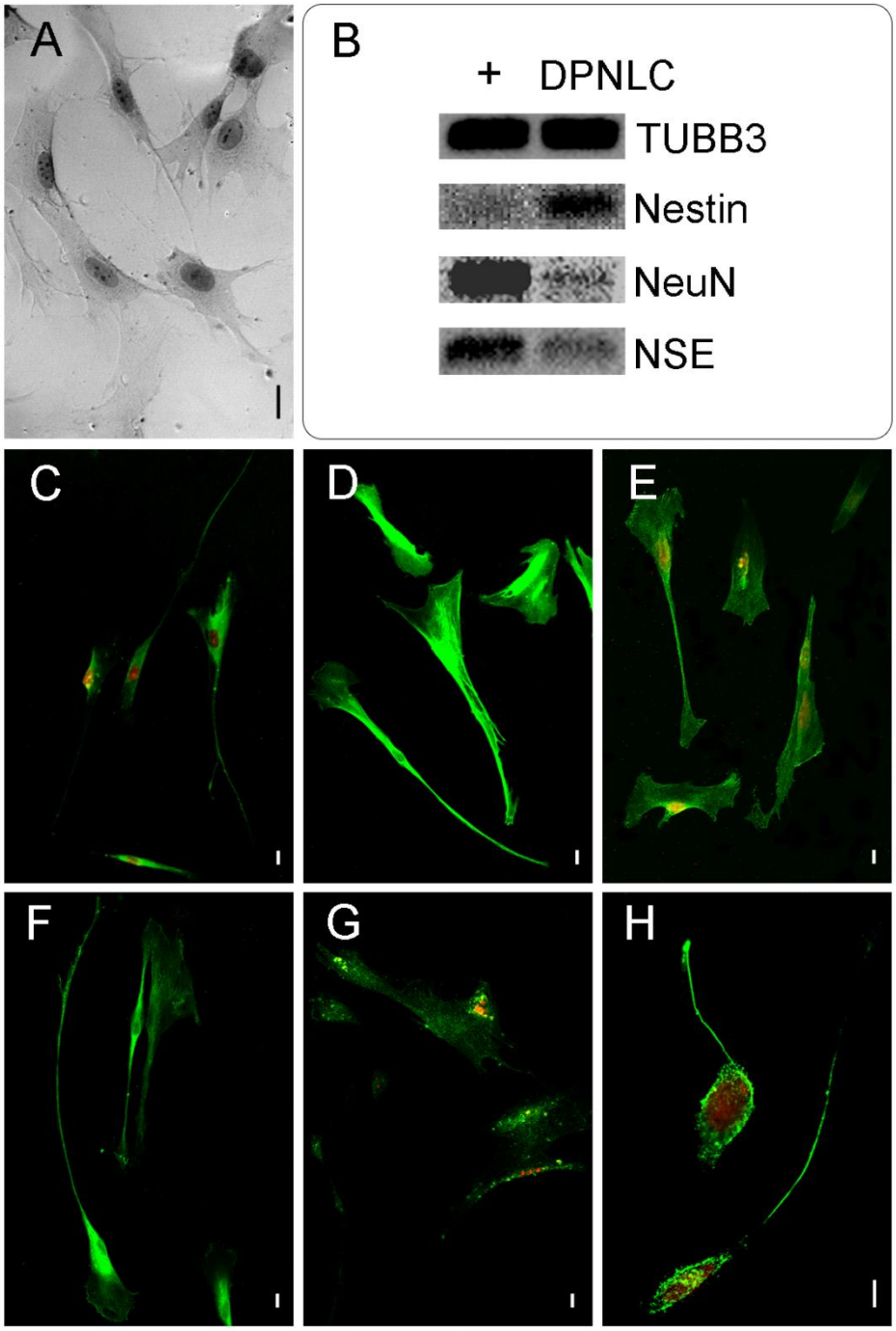

Fig.3

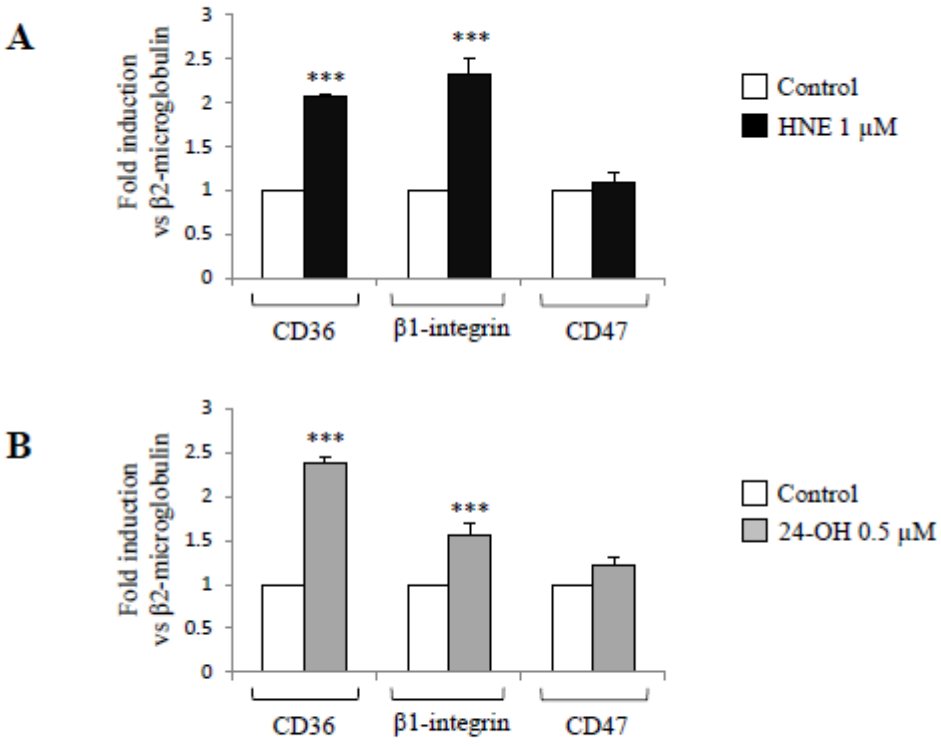
A
Fold induction vs β2-microglobulin
3
2.5
2
1.5
1
0.5
0
***
***
CD36
β1-integrin
CD47
Control
HNE 1 µM
B
Fold induction vs β2-microglobulin
3
2.5
2
1.5
1
0.5
0
***
***
CD36
β1-integrin
CD47
Control
24-OH 0.5 µM

Fig.4

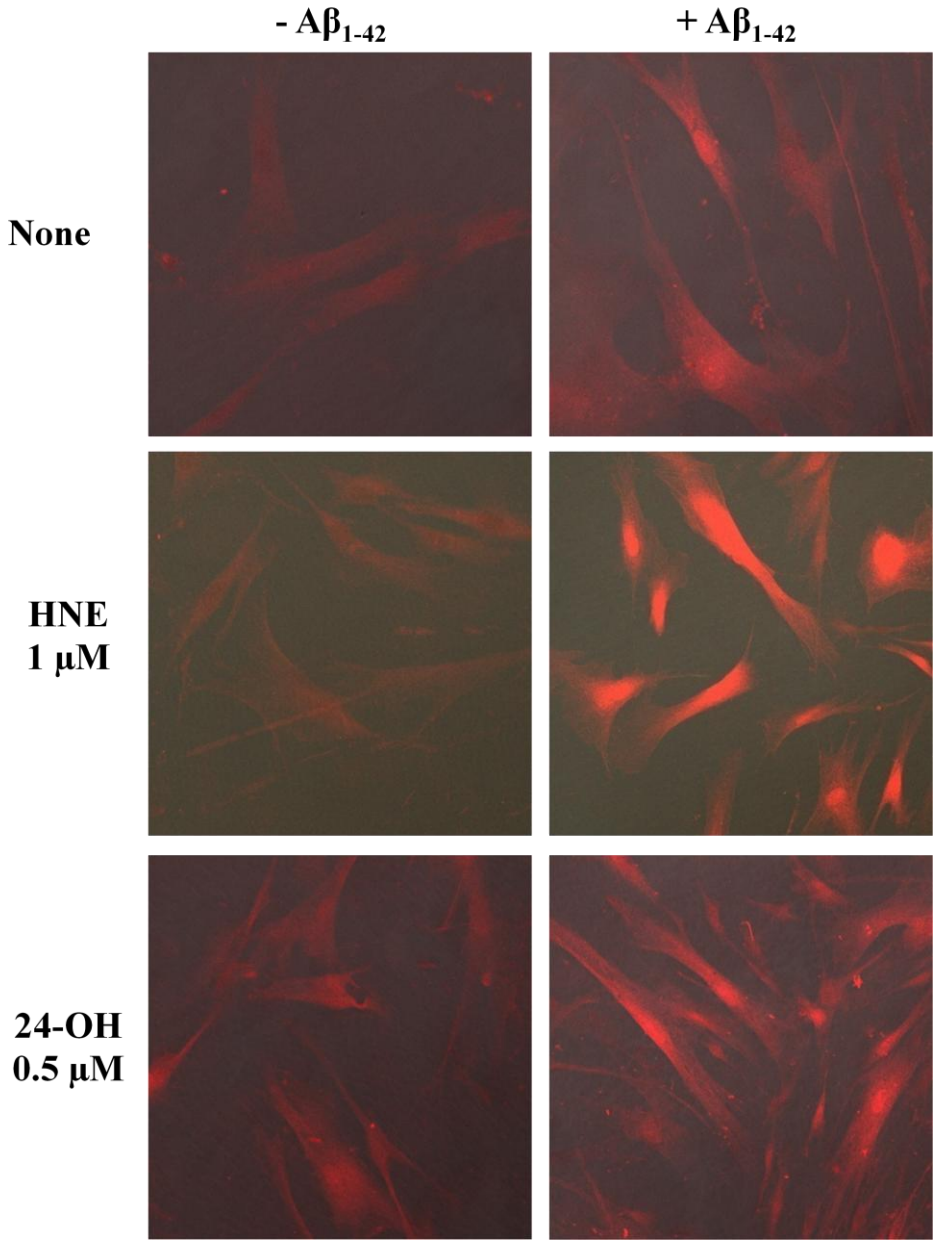

Fig.5

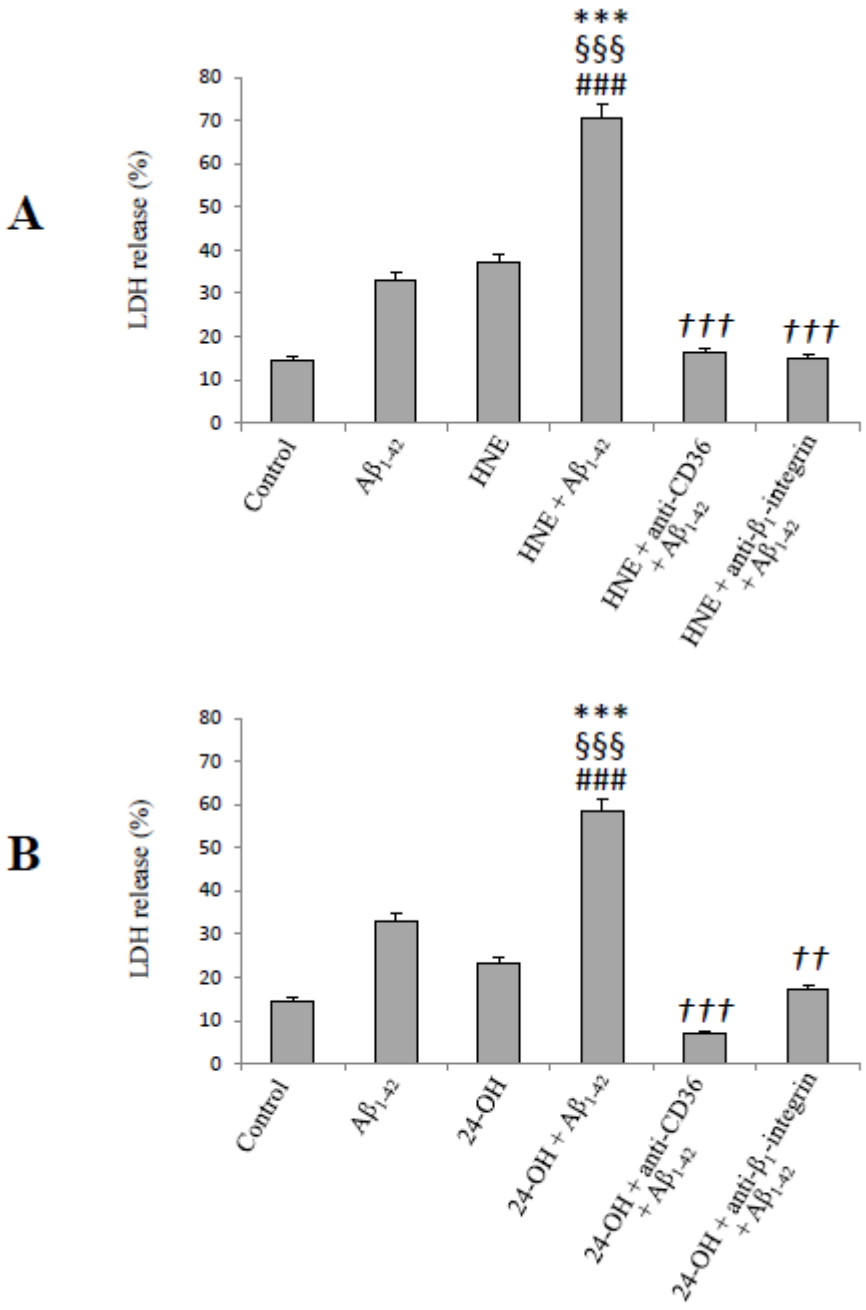
A
B
LDH release (%)
0
10
20
30
40
50
60
70
80
***
§§§
###
†††
††
Control
Aβ1-42
HNE
HNE + Aβ1-42
HNE + anti-CD36 + Aβ1-42
HNE + anti-β1-integrin + Aβ1-42
24-OH
24-OH + Aβ1-42
24-OH + anti-CD36 + Aβ1-42
24-OH + anti-β1-integrin + Aβ1-42

Fig.6

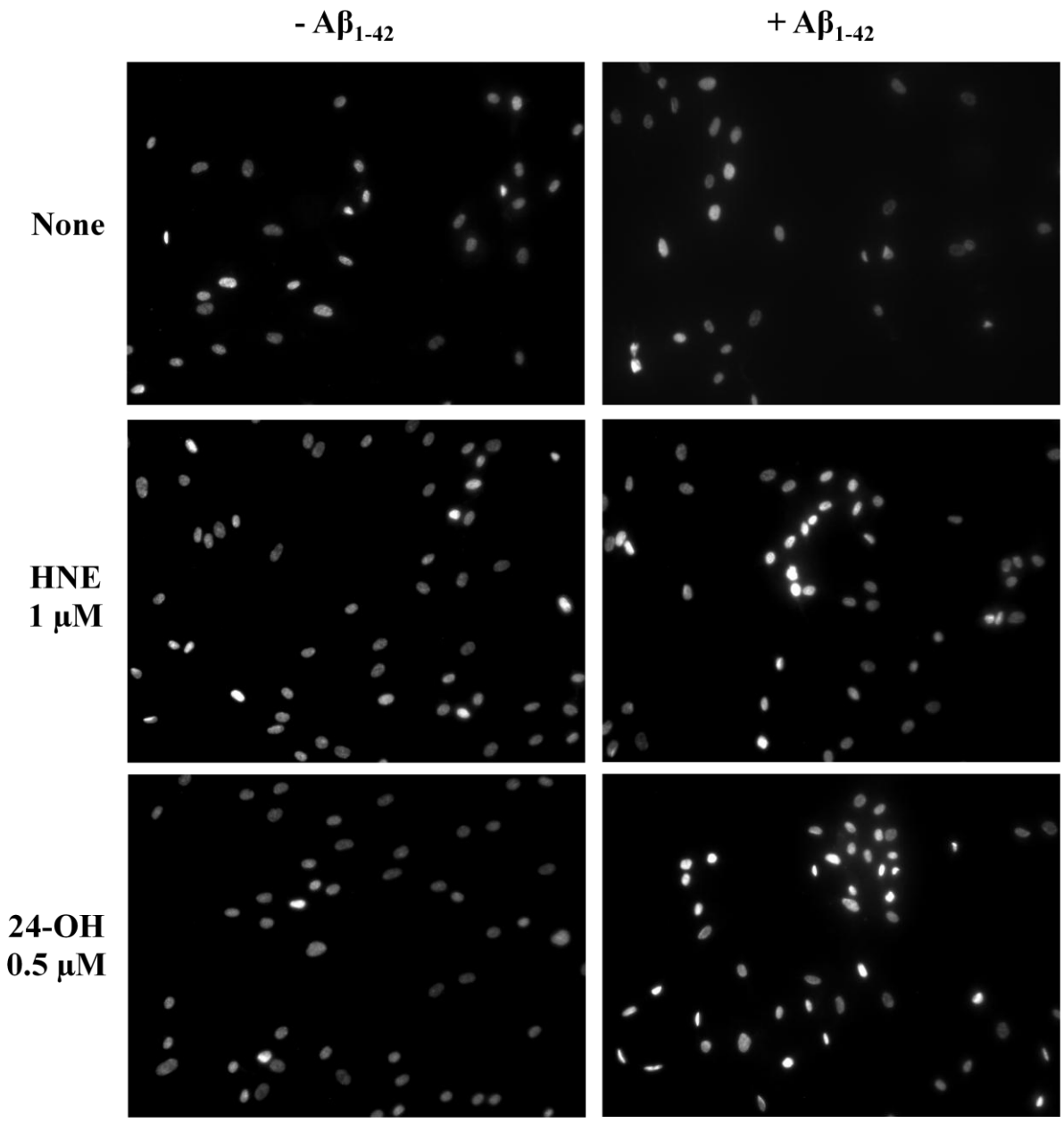

Fig.7

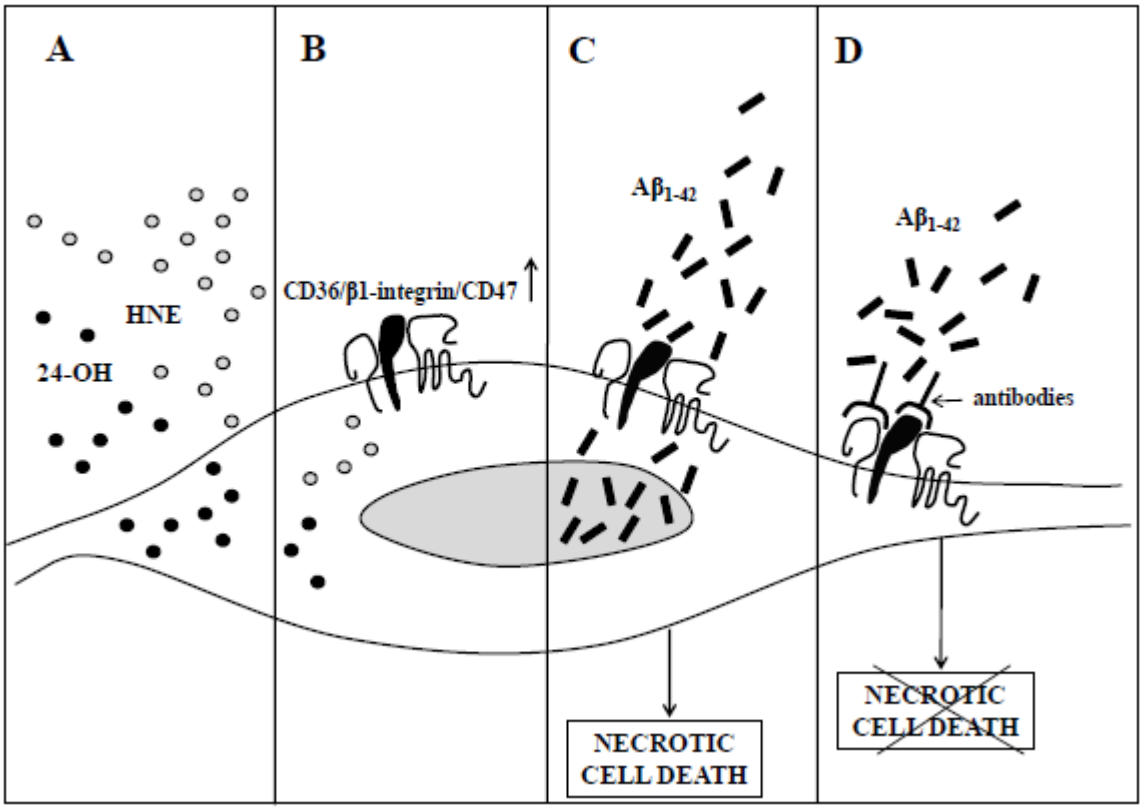
A
B
C
D
HNE
24-OH
CD36/β1-integrin/CD47
Aβ1-42
Aβ1-42
antibodies
NECROTIC CELL DEATH
NECROTIC CELL DEATH

Table 1

Table 1
Quantification of amyloid β intracellular accumulation by enzyme-linked immunoassay (ELISA).

	pg Aβ /mg proteins
Control	0.96 ± 0.2
$A\beta_{1-42}$ 200 nM	226.28 ± 25 *
24-OH 0.5 µM + $A\beta_{1-42}$ 200 nM	428.44 ± 39 *, #
HNE 1 µM + $A\beta_{1-42}$ 200 nM	450.26 ± 44 *, #

DPNLC cells were incubated for 48 h with 24-hydroxycholesterol (24-OH) or 4-hydroxynonenal (HNE) and then for 8 h with $A\beta_{1–42}$. Untreated cells were used as control. * $p<0.001$ vs. control group; # $p<0.001$ vs. $A\beta_{1-42}$.